Journal of Hydrology 487 (2013) 98–108

Contents lists available at SciVerse ScienceDirect

Journal of Hydrology

journal homepage: www.elsevier.com/locate/jhydrol

Variation of baseflows in the headstreams of the Tarim River Basin during 1960–2007

Yuting Fan [a,b], Yaning Chen [a,*], Yongbo Liu [c], Weihong Li [a]

[a] State Key Laboratory of Desert and Oasis Ecology, Xinjiang Institute of Ecology and Geography, CAS, Urumqi 830011, PR China
[b] University of Chinese Academy of Science, Beijing 100039, PR China
[c] Department of Geography, University of Guelph, Canada

ARTICLE INFO

Article history:
Received 22 November 2012
Received in revised form 14 February 2013
Accepted 16 February 2013
Available online 5 March 2013

This manuscript was handled by Geoff Syme, Editor-in-Chief

Keywords:
Baseflow
BFI
Climate change
Glacier melt
Tarim River Basin

SUMMARY

The Tarim River is the largest inland river of China and a major water resource to the vast arid region in northwest China. For its four major headstreams, which contribute 98% of the Tarim River's streamflow, we investigated the dynamics of baseflow in the past 50 years. The digital filtering method was used to separate baseflow from surface flow, after which the baseflow index (BFI) was calculated and analyzed. The major findings of this study include (1) Baseflows of the four headstreams have increased considerably over the past 50 years. The large baseflow index (BFI) usually occurred in the wet years but the change rate was irregular, because of the increasing recharge from snow and glacial meltwater. (2) The annual baseflow variation of the four headstreams appeared to have cycles of 3–5 years, 10–14 years, and 25 years. (3) The baseflow and BFI showed obvious seasonal variation: The lowest baseflow and BFI typically occurred in December and January, and both increased gradually until the maximums reached in August or July. (4) The responses of runoff and baseflow to climatic factors were different. Precipitation possessed a great impact on runoff, whereas temperature possessed a great impact on baseflow. Baseflow is an important source to the Tarim River, and is affected by the increasing snow and glaciers melt as a result of temperature rise. For the four headstreams, we identified temperature thresholds in the time series of BFI and calculated regression relationships between temperature and BFI in the past 50 years. The thresholds and the regression relationships would help to assess and predict the impact of climate change on headwater inflow to the Tarim River.

1. Introduction

Streamflow can be divided into quickflow and baseflow. Quickflow is normally from surface runoff, while baseflow is from shallow and deep groundwater. In arid inland areas, such as Xinjiang, a vast arid region located in northwestern China, baseflow becomes an important water source to support ecosystem and economic development in the region. Typically, baseflow is not very sensitive to rainfall but more associated with the discharge from groundwater. Studies have demonstrated that baseflow has a strong correlation with climate (Chen et al., 2006; Hodgkins and Dudley, 2011; Mwakalila et al., 2002). Over the past 50 years, the average temperature in Western China has increased at a rate of 0.2 °C/10 years, and about 82% of glaciers in the region have appeared retreating (Shen et al., 2006). Thus we hypothesized that the baseflows in Xinjiang had been experiencing considerable variation and would have a great impact on the regional water resource. In this study, we chose the Tarim River Basin in Xinjiang to give its baseflow variation in the past 50 years a close inspection.

The Tarim River in Xinjiang is the largest inland river of China, supporting over 20-million people, about 40% of the province's population. The total area of the river basin is 1.02×10^6 km^2. About 98% of the Tarim River's runoff is from headstreams in the upper mountain areas of the basin. The plains in the middle and downstream of the basin, receiving less than 150 mm annual precipitation, are mainly the diffusion and consumption areas and generate little surface runoff (Fu et al., 2010). About 80% of the groundwater in the basin is recharged from the surface water (Tang and Zhang, 2001). The baseflow thus does not only supply the river's runoff during the rainless season, but also recharges groundwater during the wet season. As a result, change of baseflow would greatly affect the quantity and quality of the water resources of the Tarim River, and considerably impact the human society and natural ecological environment in the region, particularly in the lower reaches of the river (Jiang and Zhou, 2007; Chen et al., 2008). However, few studies have been conducted on the

* Corresponding author. Address: State Key Laboratory of Desert and Oasis Ecology, Xinjiang Institute of Ecology and Geography, CAS, No. 818, South Beijing Road, Urumqi 830011, Xinjiang, PR China. Tel.: +86 9917823169; fax: +86 991 7823174.
E-mail address: chenyn@ms.xjb.ac.cn (Y. Chen).

0022-1694/$ - see front matter © 2013 Elsevier B.V. All rights reserved.
http://dx.doi.org/10.1016/j.jhydrol.2013.02.037

baseflow of the Tarim River Basin, including its estimation, variation, and its relation with climatic factors.

This study has three objectives: (1) To estimate baseflow quantity and baseflow index (BFI[1]) for the four major headstreams of the Tarim River (Aksu, Hotan, Yarkand, and Kaidu Rivers), using available hydrometric data and the recursive digital filtering (RDF) method; and to identify the effect of precipitation by comparing the baseflows in dry and wet years; (2) To inspect the temporal variability in the baseflows of the four rivers, by means of the Mann–Kendall test, seasonal analysis and wavelet analysis; (3) To determine the response of baseflow to climate change in the region through partial correlation and regression analyses on temperature, precipitation, baseflow, glacier melt, and seasonal variations.

2. Methods

2.1. Baseflow Separation

Typically, quickflow recession is fast and steep, whereas baseflow recession is slow and gentle in the flow process. Therefore, baseflow can be separated and estimated based on the measured flow hydrograph (Jozsef and Marc, 1998). Two types of techniques exist to disaggregate daily streamflow into quickflow and baseflow. One is the graphical separation, such as the line segmentation method and the recession curve method (Riggs, 1964); the other is the automatic methods that use computer programs to mimic the manual separation methods, such as the technique of smoothed minima (United Kingdom Institute of Hydrology, 1980), HYSEP (Sloto and Crouse, 1996) and recursive digital filtering (RDF) (Lyne and Hollick, 1979). The graphical separation methods are traditional and can be applied to different situations, but they are subjective and not suitable when data size is large. The automatic methods have been widely employed for streamflow separation with long time series. In this study, we selected the RDF technique, due to its less parameter requirement and relatively high accuracy (Hafzullah, 2009). We also implemented the traditional recession curve method to provide a performance reference.

The RDF technique, which was originally used for signal analysis and processing, became popular in hydrology literature for baseflow separation (e.g., Szilagyi, 2004; Szilagyi et al., 2005; Eckhardt, 2005, 2008). The RDF method was found to approximate well the baseflow sequence calculated by the manual separation technique using matching strips (Nathan and McMahon, 1990). RDF smoothes sharp peaks in the fast component of the streamflow, so that the separated flow represents the delayed component of the streamflow, i.e., the baseflow (Lyne and Hollick, 1979). The RDF process can be represented as

$$Q_d(t) = \beta Q_d(t-1) + (1+\beta)/2[Q(t) - Q(t-1)] \quad (1)$$

where Q_d (m^3/s) is the filtered quick streamflow; Q (m^3/s) is the total streamflow; t is the time step (day), and β is a filter parameter. The filtered baseflow Q_b can then be obtained by:

$$Q_b(t) = Q(t) - Q_d \quad (2)$$

Most acceptable results were obtained when β was in the range 0.90–0.95, with an optimal value as 0.925 (Nathan and McMahon, 1990). The algorithm separates baseflow from total streamflow by passing the filter over the streamflow record three consecutive times (forwards, backwards, and forwards again). Each filter pass produces three time series estimates of baseflow, with the last being the projected baseflow time series. Justification for the use of this method rests on the fact that filtering out high-frequency signals is intuitively analogous to the separation of low frequency baseflow from the higher frequencies of quickflow (Nathan and McMahon, 1990). The output of the filter is constrained such that the separated flow cannot take negative values and is not greater than the total flow.

The recession curve method is the main traditional graphical separation method. It has been used to separate surface flow from total flow, and the derived groundwater flow is considerably higher during flood events than that during dry seasons (Tallaksen, 1995; Hafzullah et al., 2009). The recession curve method has an advantage of flexible adjustment for the basin characteristics, but is tedious and time-consuming for baseflow separation with a long time series. In this study, it was implemented as a performance benchmark to the RDF.

The recession curve method can be expressed as:

$$Q_t = Q_0 K^{-t} \quad (3)$$

where Q_t (m^3/s) is the discharge at any tie step t; Q_0 (m^3/s) is the discharge at the initial time step; and K is the recessions constant.

The BFI is one of the most important low flow indexes, which is the long-term ratio of baseflow volume to total streamflow volume, and affected by a number of climatic and topographic factors (Antonia and Paolo, 2008). Therefore, it can be used to analyze the correlation between baseflow and climate factors. BFI is calculated as a ratio between baseflow volume and total streamflow volume for a time period, and can be expressed as:

$$\mathrm{BFI} = \frac{\int_{t_1}^{t_2} Q_b(t)dt}{\int_{t_1}^{t_2} Q(t)dt} \quad (4)$$

where t_1 and t_2 are starting and ending time points, respectively. In our study area, winter baseflow is less related to the winter precipitation. Snowfall is accumulated from December to February and supplies baseflow during the spring snowmelt season. To study the variation of winter baseflow, the stable BFI (SBFI[2]) is defined as the ratio of winter baseflow volume to the total yearly streamflow volume, and is expressed as:

$$\mathrm{SBFI} = \frac{\int_{t_D}^{t_F} Q_b(t)dt}{\int_{t_D}^{t_N} Q(t)dt} \quad (5)$$

where t_D, t_F, and t_N are the months of December, February, and November, respectively. The recession curve method was applied to the Kaidu River for a comparison with the RDF method. The calculated BFI difference between the two methods varies with β, and reached its minimum when β is 0.925.

2.2. Time series analysis

2.2.1. Trend detection

In this study, we used the Mann–Kendall test to detect the monotonic trend of baseflow and BFI. This method has a high asymptotic efficiency and is able to handle non-normality, missing values, and those data reported as "less than" in the dataset (Burn, 1994; Xu et al., 2003). The null hypothesis for the trend test that there is no increasing/decreasing trend present. The equation of Mann–Kendall test can be expressed as

$$Z = \begin{cases} \frac{S-1}{\sqrt{var(S)}}, & S > 0 \\ 0, & S = 0 \\ \frac{S+1}{\sqrt{var(S)}}, & S < 0 \end{cases} \quad (6)$$

where

[1] BFI is calculated as a ratio between baseflow volume and total streamflow volume for a time period.

[2] SBFI is defined as the ratio between winter baseflow volume and the total yearly streamflow volume.

$$Var(S) = [n(n-1)(2n+5) - \sum_t t(t-1)(2t+5)]/18 \quad (7)$$

$$S = \sum_{i=1}^{n-1} \sum_{k=i+1}^{n} sgn(x_k - x_i) \quad (8)$$

and

$$sgn(\theta) = \begin{cases} 1, & \theta > 0 \\ 0, & \theta = 0 \\ -1, & \theta < 0 \end{cases} \quad (9)$$

where x_k, and x_i are the sequential data values, n is the length of the data set, and $sgn(\theta)$ is a sign function. The null hypothesis, H_0, is accepted if the test statistic Z is not statistically significant, i.e. $-Z_{1-\alpha/2} \leqslant Z \leqslant Z_{1-\alpha/2}$, in which $\pm Z_{1-\alpha/2}$ are the standard normal deviates, and α is the significance level for the test. Correspondingly, the presence of a trend is accepted if Z is statistically significant if $Z < -Z_{1-\alpha/2}$ or $Z > Z_{1-\alpha/2}$.

2.2.2. Seasonal analysis

Seasonal analysis is used to identify seasonal trend, fluctuation, periodicity, and irregular variations in the time series (Men and Yan, 2002; Jiang and Xia, 2007). If peak values appear in the same season in each year and trough values appear in another same season, we can assume that the data have a seasonal pattern. The goal of the seasonal decomposition procedure is to extract a seasonal component and a combined trend-cycle component from the observed signal, assuming the residual as the "error" component. In the present study, we used monthly baseflow data to conduct seasonal analysis and inspected seasonality of the time series based on a 12-months cycle. The seasonal index (S_k), which indicates the seasonality for a given time period in a year, was calculated. S_k is typically represented by the ratio of the mean of observed value in a certain period of a year for many years to what it would be if no seasonal variation is present. S_k can be calculated as:

$$S_k = \frac{\overline{x_k}}{\bar{x}}, \quad k = 1, 2, \ldots, m \quad (10)$$

where $\overline{x_k}$ is the average of the observed values from many years for the same period:

$$\overline{x_k} = \frac{\sum_{i=1}^{n} x_{ik}}{n}, \quad k = 1, 2, \ldots, m \quad (11)$$

where k indicates the same period from different years; n indicates the length of the entire time series; m indicates the number of the periods in a year; and $\bar{x}$ is the average of the entire time series:

$$\bar{x} = \frac{\sum_{i=1}^{n} \sum_{k=1}^{m} x_{ik}}{nm} \quad (12)$$

If seasonality is absent, baseflow would fluctuate randomly around the average on monthly basis. Otherwise, monthly baseflow would present similar patterns in different years. $S_k > 1$ means that the value of the given period in a year is often higher than the overall average, and $S_k < 1$ indicates that the value of the period is often lower than the overall average. If S_k has large variance, and the extreme value is not close to 1, it indicates that this sequence has considerable seasonal efficiency. In other words, a strong seasonality exists if S_k value is far away from 1.

2.2.3. Wavelet analysis

Wavelet transform is a multi-resolution tool for signal analysis. It dilates and translates the original wavelet function $\psi(t)$ (Dai, 2000):

$$\psi_{a,\tau}(t) = \frac{1}{\sqrt{a}} \psi\left(\frac{t-b}{a}\right) a, \quad \tau \in R, \quad a > 0 \quad (13)$$

The Morlet wavelet was a function applied to the continuous wavelet transform. It can make the wavelet has good concentration in the frequency domain and time domain. In our study, The Morlet wavelet was selected to do transform. The Morlet wavelet function is given as:

$$\psi(t) = e^{ict} e^{-t^2/2} \quad (14)$$

The original signal can be reconstructed by the wavelet decomposition coefficient $W_f(a, b)$,

$$W_f(a,b) = \frac{1}{a} \int (t) \psi^* \left(\frac{t-b}{a}\right) dt \quad (15)$$

In above three equations, a and b denote the scale and shift parameters, respectively; t is the original signal; τ is displacement factor; R is the real number set; c is a constant; i is the imaginary part; and * represents the conjugate operator. The noise signal is then separated into frequency and time regions based on the values of a and b.

2.2.4. Partial correlation

When evaluating the correlation between two variables, if it is known that one or both of the variables are correlated to a third variable, partial correlation analysis can be used to remove the impact of the third variable and reveal the unique correlation between the two considerable variables. In this study, we used partial correlation to evaluate the relationships between two river factors and two climate factors. The two river factors are runoff and baseflow, and the two climate factors are precipitation and temperature. When evaluate the relationship between a river factor and a climate factor (e.g. precipitation), we consider the other climate factor (e.g., temperature) as the third factor in the partial correlation calculation. The first-order partial correlation is defined as:

$$r_{y1,2} = \frac{r_{y1} - r_{y2} r_{12}}{\sqrt{\left(1 - r_{y2}^2\right)\left(1 - r_{12}^2\right)}} \quad (16)$$

where r_{y1}, r_{y2}, and r_{12} stand for the correlation coefficients between y and x_1, y and x_2, and x_1 and x_2, respectively. The physical meaning of $r_{y1.2}$ is the correlation between the parts of x_1 and y that are uncorrelated with x_2 (Fuente et al., 2004). For example, for the correlation between runoff and precipitation in our case, y is runoff; x_1 is precipitation; x_2 is temperature; and $r_{y1.2}$ is the partial correlation between runoff and precipitation. For the case between runoff and temperature, temperature becomes x_1, and precipitation becomes x_2. Similarly x_1 and x_2 can be defined for the cases between baseflow and precipitation, and between baseflow and temperature. The partial correlation coefficient ranges from −1 to +1. A positive $r_{y1.2}$ indicates a positive linear relationship between the two variables, and a negative $r_{y1.2}$ indicates a negative linear correlation between the two variables.

3. Study area

The Tarim River Basin, with a drainage area of 1.02×10^6 km^2, is the largest inland river basin in China. The majority of the basin is located in Xinjiang, the largest provincial administration unit of China, and occupies about two thirds of the total area of Xinjiang. The Basin is composed of 114 streams belonging to nine river systems, including the Aksu River, Kashgar River, Yarkand River, Hotan River, Kaidu River, Dina River, Weigan River, Kuqa River, and Keriya River. The landforms of the Tarim River Basin include mountains (47%), plains (22%), and deserts (31%) (Xie et al., 2007). The Aksu River, Yarkand River, and Hotan River join the Tarim River at its upper reaches, while the Kaidu River flows into the Tarim River at the lower reaches. The Tarim River Basin has a typical

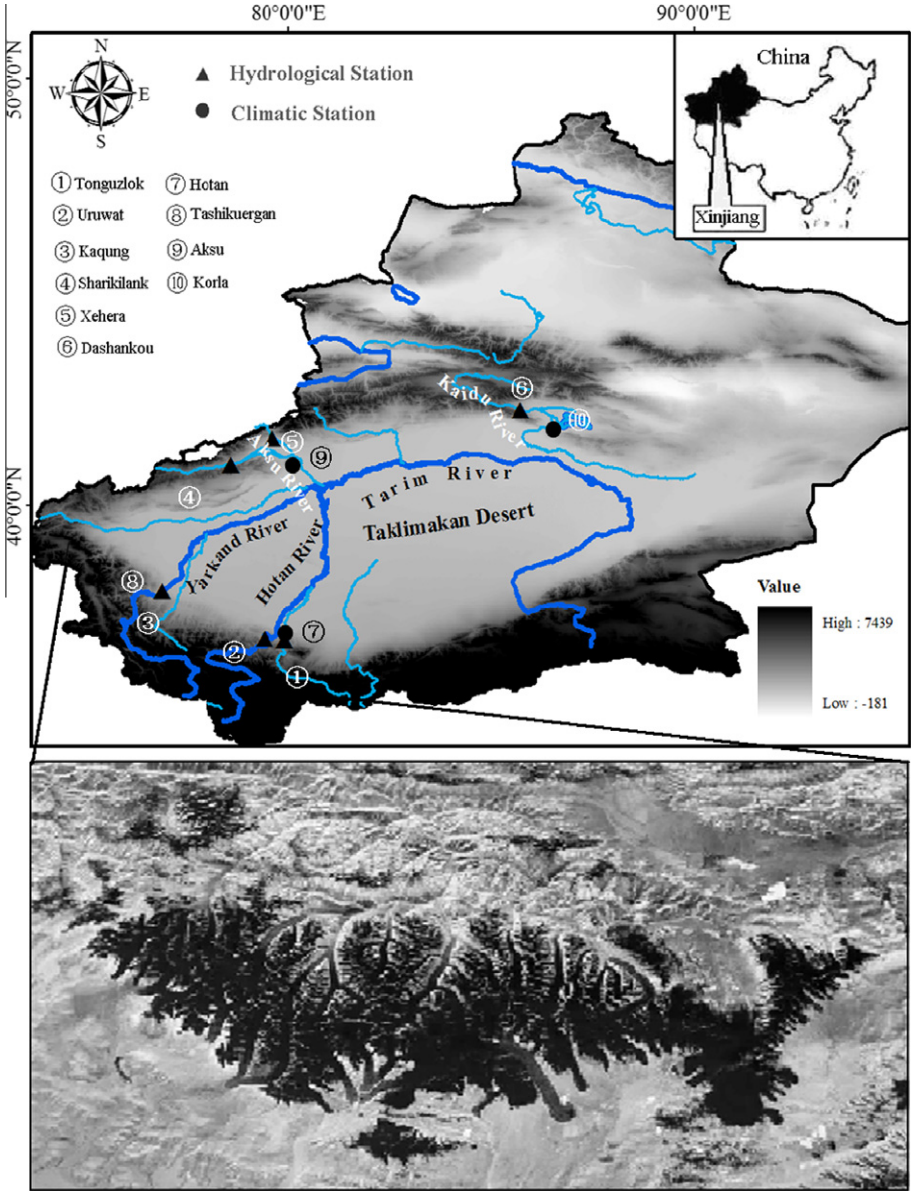

Fig. 1. The Tarim River and its headstreams. The following figure is a map of the Kunlun Mountains glacier. Snow line is at an altitude of 5600–5900 m.

Table 1
Catchment and baseflow characteristics of the four headwater streams.

River	Drainage area (km^2)	Average elevation (m)	Average baseflow (10^8 m^3)	Standard deviation (10^8 m^3)	Median baseflow (10^8 m^3)
Aksu River	35,871	7435	3.99	1.05	3.58
Hotan River	48,870	6000	1.91	0.37	1.79
Yarkand River	48,100	5395	12.31	1.25	12.45
Kaidu River	22,000	4679	10.79	2.29	10.54

continental climate, as it is far away from the ocean and surrounded by high mountains. The regional climate is extremely dry, with little precipitation and strong potential evaporation (Chen and Xu, 2005). The mainstream of the Tarim River is about 1321 km in length, from the confluence composed of the Aksu, Hotan, and Yarkand Rivers to the Taitema Lake (Fig. 1).

In the headwater areas of the Tarim River, there are 11,711 glaciers in the surrounding mountains with a total area of 19,889 km^2 and a total volume of 2313 km^3 (Shen et al., 2006). In the catchments of the three most important headstreams of the Tarim River, namely the Aksu River (northwest of the Basin), the Hotan River (East of the Basin), and the Yarkand River (southwest of the Basin), glaciers account for 75% of the total water storage in the basin and is a major water source to the upper reaches of the Tarim River (Shi, 2005).

The four headstreams catchments were selected for this study. Daily discharge data of the four streams from 1960 to 2007 are available at six stations located upstream to where the streams join the mainstream of the Tarim River. Daily temperature and precipitation data are available at four climate stations in the area, and we obtained them from the China Meteorological Data Sharing Service System (http://cdc.cma.gov.cn). The map of the west Kunlun

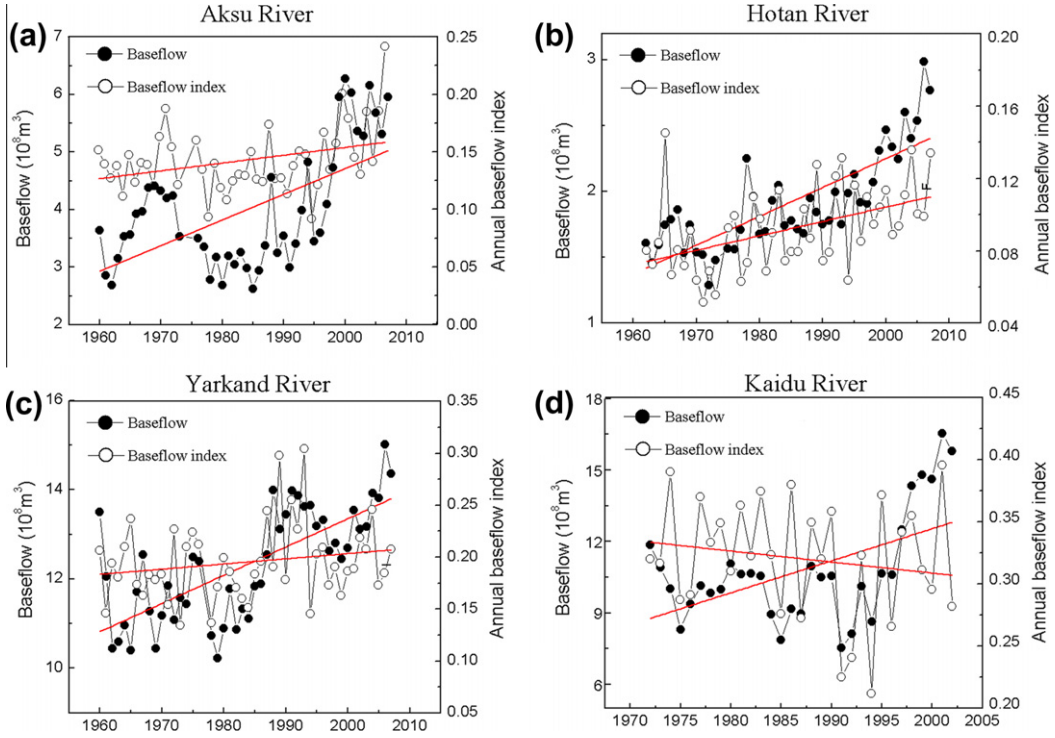

Fig. 2. Variation of annual baseflow and baseflow index for the four headstreams of the Tarim River.

Table 2
Annual variations of baseflow and BFI for the four headwater streams.

River	Baseflow and BFI	1960–1969	1970–1979	1980–1989	1990–1999	2000–2008
Aksu	Q_b (10^8 m^3)	3.61	3.63	3.19	4.06	5.75
	BFI (%)	13.37	14.42	13.12	13.49	17.62
Hotan	Q_b (10^8 m^3)	1.66	1.65	1.80	1.96	2.54
	BFI (%)	8.65	7.52	9.21	9.80	10.95
Yarkand	Q_b (10^8 m^3)	11.39	11.44	11.94	13.30	13.70
	BFI (%)	18.73	18.38	19.81	20.50	20.16
Kaidu	Q_b (10^8 m^3)	/	10.06	9.93	10.79	/
	BFI (%)	/	33.23%	32.94%	30.05%	/

Q_b is the baseflow, BFI is the baseflow index.

Mountains glacier was provided by the Environmental and Ecological Science Data Center for West China (http://westdc.westgis.ac.cn). The locations of the climate and hydrological stations that served the data used in this study are shown in Fig. 1.

4. Result and discussion

4.1. Baseflow separation

Table 1 presents the catchments and estimated baseflows of the four headstreams, as well as their characteristics. The annual average SBFI of baseflow are 0.13 (Aksu River), 0.08 (Hotan River), and 0.23 (Yarkand River) to upstream Tarim River, and 0.36 (Kaidu River) to the downstream Tarim River. The calculated baseflow increasing rates of the four rivers are 14.1%, 6.9%, 20.1%, and 42.6%, respectively (Fig. 2). The SBFIs of the Aksu River and Hotan River show continuously increasing trends, whereas the Yarkand River is featured by fluctuations, and the Kaidu River shows a decreasing trend (Fig. 2). Table 2 presents the estimated baseflows and the corresponding SBFI in different decades. In terms of the relationship between baseflow amplitude and SBFI, each river has its unique characteristic. From 1980s to 1990s, the rising amplitude of Aksu River's baseflow is not proportional to the SBFI; from 1970s to 1980s, the declining amplitude of Hotan River baseflow is not proportional to the SBFI; around 1970 and in 2000, the Yarkand River's baseflow increased but SBFI decreased; the Kaidu River's baseflow first decreased, and then increased, while the SBFI has been declining all the time (Table 2). It is speculated that climatic factors have been play a role in the relationship between baseflow amplitude and SBFI.

Over the past 50 years, the SBFI of the Hotan River, Yarkand River, and Kaidu River were 8.0–30.1% of the streamflow in dry years (we define that a year with annual precipitation less than 40 mm is a dry year), and 10.8–37.0% in wet years (annual precipitation is more than 100 mm) (Fig. 3). If the baseflow of a river is relatively constant, when the precipitation-supplied runoff increases, the proportion of baseflow in the entire streamflow should decrease. However, the SBFI of the Hotan River, Yarkand River, and Kaidu River appeared generally larger in wet years than in dry years (Fig 3). Tetzlaff and Soulsby (2008) concluded that BFI is larger in dry years than in wet years based on a study in mountainous regions underlain by crystalline basement rocks and metamorphic formations with small aquifer potentials. In that kind of area, because of the limited storage in superficial deposits and thin soils, precipitation becomes surface runoff and enters streams directly instead of deep percolation. In our study area, we see an opposite scenario, i.e., larger SBFI in wet years. An explanation to this uncommon phenomenon is that the increasing glacial meltwater had raised the level of baseflows in the rivers during those wet years, which is an outcome of a warm–wet condition. In the past 48 years, the warming–wetting trend in the Tarim River Basin should be a regional response to the global climate change, and the 1990s is the decade with the highest annual temperature (Chen et al., 2009). Baseflows of Aksu, Hotan and Kaidu Rivers began to increase in 1990s, and baseflows of Yarkand River began to increase in the late 1990s.

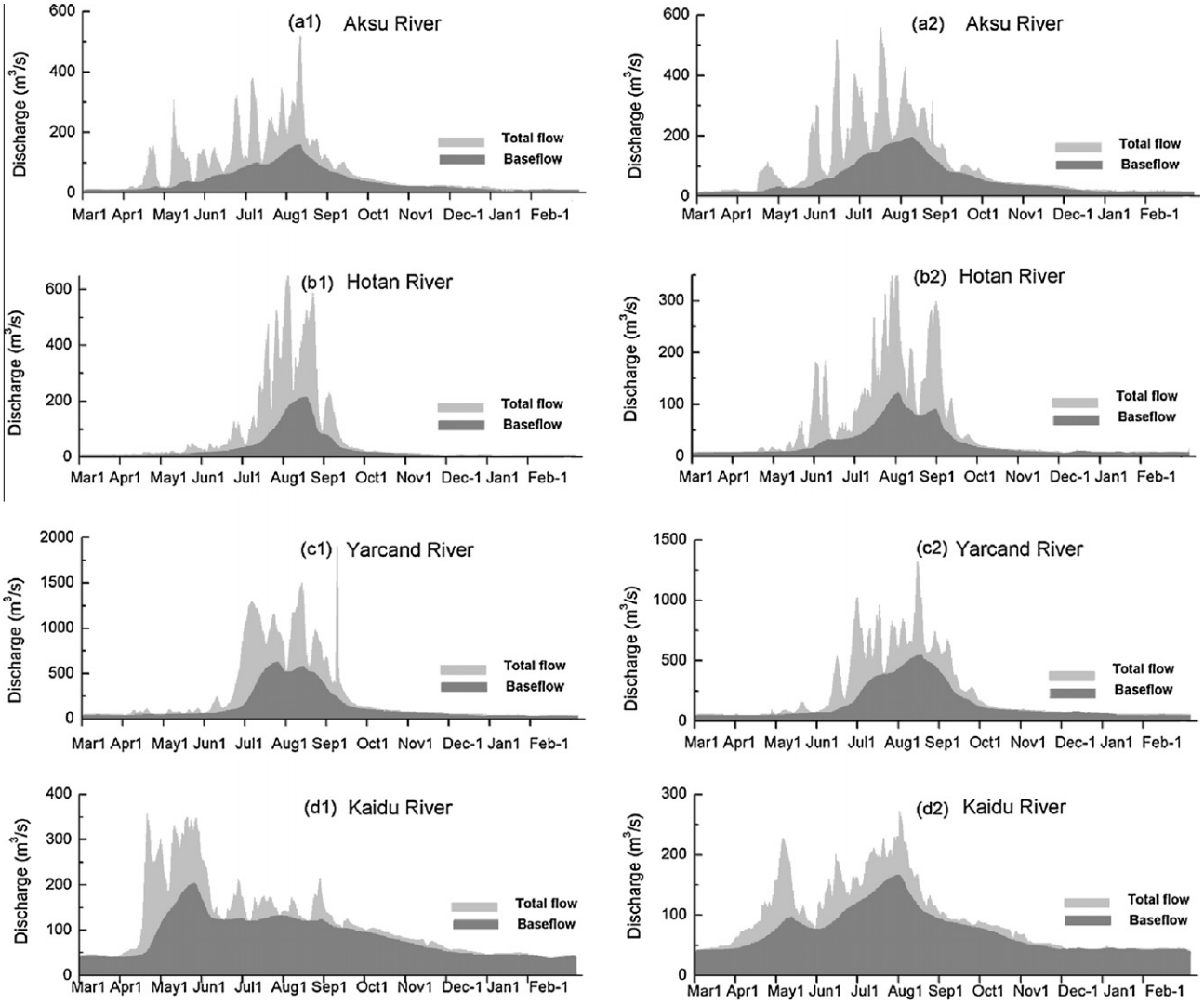

Fig. 3. Baseflow separation at the four headstreams of the Tarim River for typical dry and wet years: (a1) Aksu River in a dry year 1986 with SBFI = 12.7%, (a2) Aksu River in a wet year 1996 with SBFI = 12.5%, (b1) Hotan River in a dry year 1985 with annual SBFI = 8.0%, (b2) Hotan River in a wet year 1987 with SBFI = 10.8%, (c1) Yakand River in a dry year 1978 with SBFI = 13.0%, (c2) Yakand River in a wet year 2007 with SBFI = 21.5%, (d1) Kaidu River in a dry year 1980 with SBFI = 30.0%, and (d2) Kaidu River in a wet year 1981 with SBFI = 37.0%.

4.2. Time series analysis of baseflow and BFI

Table 3 presents the results of trend analysis on baseflow and BFI for the four headwater streams. For the Aksu River and Hotan River, both baseflow and BFI show monotonic increasing trends. For the Yarkand River and Kaidu River, their baseflows show monotonic increasing trends, whereas the BFIs do not.

Fig. 4 shows the wavelet analysis results of the annual baseflow time series of the four rivers over the past 50 years. We also show wavelet analysis results of the annual temperature time series in order to further validate the periodicity of baseflow. The results represent the characteristics of the baseflows in various time scales, and the temperature has a similar wavelet cycle distribution pattern with baseflow. The wavelet coefficient represents the correlation between the wavelet and the signal. The light areas in the figure represent the baseflows above the normal level (positive), and the dark areas represent the baseflows below the normal (negative). The Aksu River's annual baseflow fluctuation has three major frequencies: 5 years, 14 years, and 25 years; The Hotan River has frequencies of 3 years, 13 years, and 25 years; The Yarkand River has frequencies of 3 years, 10 years, and 26 years; and the Kaidu River has one major frequency of 17 years. The 10–15-year scales were obvious after 1970. Those smaller oscillations (less than 12 years) have more positive and negative alternate periods. When we analyzed the wavelet coherence between the temperature and baseflow, oscillations in temperature are manifested in the baseflow on wave lengths, varying from 2 to 4 years for Aksu, Hotan and Yarkand Rivers, and 8–9 years for Kaidu River, suggesting that baseflow passively mirrors temperature.

We developed a seasonal adjustment model with a cycle = 12 - months to calculate the seasonal factor for each month. The results show that the baseflow has an apparent seasonal pattern, i.e. small baseflow occurs in December and January with a low seasonal index. They both gradually increase from February to July until their maximums are reached in summer, and then drop from summer to winter. The lowest seasonal factor of Aksu, Hotan, Yarkand and Kaidu Rivers is 0.18, 0.15, 0.24 and 0.35 in January, respectively; and the largest seasonal factor of Aksu, Hotan, and Yarkand Rivers is 2.73, 4.03, and 3.65 in August, respectively, and for Kaidu River it is 1.96 in July. The increase in baseflow occurs during the melting seasons, and an explanation to this seasonal pattern is that the baseflow is from groundwater recharged by precipitation and

Table 3
Monotonic trend test of baseflow and BFI for the four headstream streams.

Diagnosis		Aksu River		Hotan River		Yarkand River		Kaidu River	
		Q_b	BFI	Q_b	BFI	Q_b	BFI	Q_b	BFI
Mann–Kendall	Z_0	3.503	1.856	6.016	3.453	5.044	1.155	2.074	−0.68
	H_0	R	R	R	R	R	A	R	A

Q_b is the baseflow, BFI is the baseflow index.

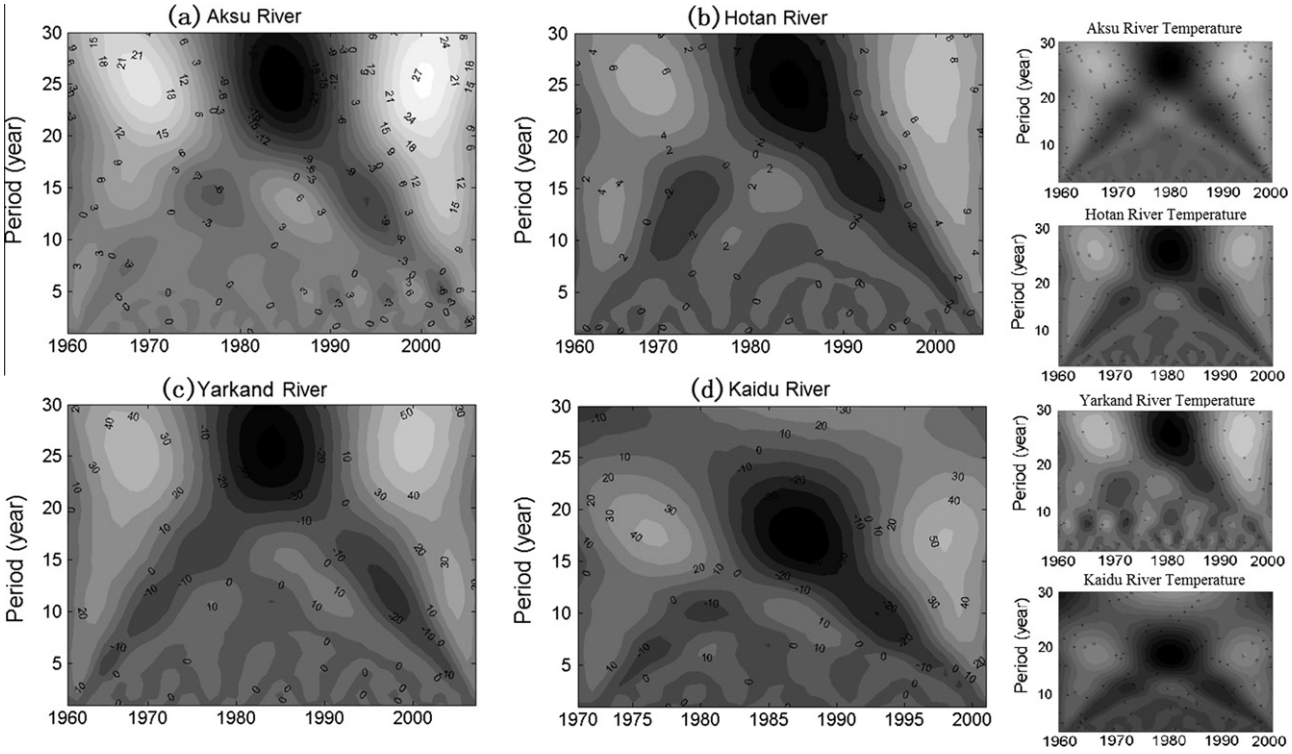

Fig. 4. Wavelet analysis of annual baseflows for the four headstreams of the Tarim River.

glacier meltwater, and therefore affected by both precipitation and temperature. As a result of temperature rise and glacier retreatment, streamflow in the region has been increased over the past years (Liu et al., 2006). The maximum monthly mean streamflow is observed in summer months (Table 5) when the rates of baseflow and groundwater recharge are also at their maximum. In late fall and winter months, all terms are reduced and streamflow is mainly from baseflow.

4.3. Responses of baseflow to the changes of climatic factors

4.3.1. Correlation between climatic factors and baseflow

The partial correlation analysis reveals that the variability of the annual and seasonal baseflow and SBFI has a close relationship with climatic factors. As presented in Table 4, the temperature has a noticeable relationship with precipitation. A positive relationship between temperature and precipitation was found for the Aksu River, whereas negative relationships were found for the Hotan, Yarkand and Kaidu rivers.

Precipitation has a great positive impact on the runoff of the Aksu River and Kaidu River, but a considerable negative impact on the runoff of the Hotan River. Temperature has a great positive impact on the runoff of the Yarkand River. When the impact of temperature is controlled, precipitation still has a great positive impact on the runoff of the Aksu River and Kaidu River, and a considerable negative impact on the runoff of the Hotan River, but its impact on runoff of the Yarkand River becomes small. When the impact of precipitation is controlled, the partial correlation between temperature and runoff of the Yarkand River is weakened, and there is no apparent impact of temperature on the runoff of the other three rivers.

In terms of baseflow, temperature has a great positive impact on all four rivers. When the impact of temperature is controlled, precipitation has a small positive impact on the baseflows of the four rivers. When the impact of precipitation is controlled, the partial correlation between the temperature and baseflows of the Aksu River is weakened, but the partial correlation between temperature and baseflows of the Hotan River, Yarkand River and Kaidu River are strengthened. So temperature has a large positive impact on the baseflows of the Hotan River, Yarkand River and Kaidu River, and a little positive impact on the baseflow of the Aksu River.

For the SBFI, temperature has a great positive impact on the Aksu River and Hotan River, and precipitation has a large positive impact on the Yarkand River. When the impact of temperature is controlled, precipitation has a small negative impact on the SBFI of the Aksu River and Kaidu River, and a small positive impact on the SBFI of the Hotan River and Yarkand River. When the impact of precipitation is controlled, temperature has a considerable positive impact on the SBFI of the Aksu River and Hotan River, a small positive impact for the Kaidu River, and a small negative impact for the Yarkand River.

Table 4
Partial correlation analysis between flow variables (runoff, baseflow, and BFI) and climate factors (temperature and precipitation) for the four rivers.

Item	Correlation and partial correlation	Aksu River	Hotan River	Yarkand River	Kaidu River
P	Correlation T	0.466	−0.367	−0.351	−0.535
Runoff	Correlation P	0.410**	−0.393**	−0.147	0.515***
	Correlation T	0.23	−0.079	0.276*	0.255
	Partial correlation P	0.369**	−0.398**	None	0.468***
	Partial correlation T	None	None	0.266	None
Baseflow	Correlation P	0.252	0.144	0.221	0.099
	Correlation T	0.650**	0.680**	0.145*	0.572**
	Partial correlation P	0.275	0.259	0.269	0.045
	Partial correlation T	0.656	0.698***	0.212*	0.567***
BFI	Correlation P	0.015	0.086	0.344*	−0.038
	Correlation T	0.496**	0.316*	−0.22	0.048
	Partial correlation P	−0.021	0.113	0.305	−0.027
	Partial correlation T	0.497	0.323	−0.147	0.041

* Significance at the level of $P < 0.05$ (2-tailed).
** Significance at the level of $P < 0.01$ (2-tailed).
*** Significance at the level of $P < 0.001$ (2-tailed).

Table 5
Glacier storage of the four Headstream Rivers and the seasonal distribution of runoff in 1960s.

River	Glacier-ID	Glacier storage		Distribution of runoff (%)			
		km^3	%	Spring	Summer	Autumn	Winter
Aksu River	5Y67	436.99	18.89	13.5	64.3	17.3	4.9
Hotan River	5Y64	578.71	25.02	8.0	74.8	12.8	4.4
Yarkand River	5Y65	612.10	26.46	8.4	70.3	15.9	5.4
Kaidu River	5Y69	23.25	1.01	24.7	37.9	22.2	15.2

The % in glacier storage is the component of the total Tarim River.

Chen et al. (2009) found that precipitation increased significantly in Tarim River Basin during the last 50 years. The annual precipitation at the Aksu River decreased during the period from the 1960s to the 1970s; then became increasing and reached the multi-annual average in the 1980s; it increased by 18.9% in the 1990s. The change in precipitation at the Hotan River was not so drastic, which is about 10%, with increase in summer and autumn, decrease in spring, and no significant change in winter. The annual precipitation at the Yarkand River in the 1970s was the lowest, and then began to increase from the 1980s and increased by 20.7% in the 1990s. The annual precipitation at the Kaidu River was dominated by slight negative anomaly during the period from the 1960s to the 1980s, and significantly increased since the 1990s. Chen et al. (2009) concluded that the arid climatic environment in the drainage basin cannot be qualitatively changed by a short-term precipitation increase due to the peculiar geographical location and the climatic conditions. Compared with precipitation, it appears that temperature has a stronger correlation with baseflow, which may indicate that temperature is a more important factor in controlling baseflow in the four headstreams of the Tarim River.

4.3.2. Response of glaciers to the temperature increase

The large storage of glaciers in the four headstream catchments was reported in 1960s (Shi and Xie, 1964) (Table 5). The biggest glacier in Tianshan Mountain, the Yiliqier glacier, is located in the source region of the Kunma Lectra River, the largest tributary of the Aksu River. According to the record of Xiehera Hydrological Station, the runoff of the Aksu River increased by 25% in 1990s, compared with the runoff in 1950s (Shen et al., 2006). Aerial mapping in 1970 and satellite imageries in 1989 and 2001 show that the glaciers at the Yulong Kashi River, the main tributary of the Hotan River, changed from expansion to shrinkage, and this shrinkage has accelerated since 1989 (Shi, 1990). From 1960 to 1995, the ratio of glacier meltwater to total runoff in the Yarkand River increased from 50% to 80% (Shi, 2005).

Based on the data collected at the hydrological stations of the four Headstream Rivers, the seasonal distributions of surface runoff of these rivers were highly variable (Table 5). For the Aksu, Hotan, and Yarkand rivers, the summer (June–August) runoff accounts for 60–75% of the yearly runoff, and the spring runoff accounts for 8–13.5%. The Kaidu River is primarily supplied by spring snow and glaciers melt, so the amount of its spring (March–May) and summer (June–August) runoff accounts for 62% of the yearly runoff. In spring and summer, glaciers contribute 150×10^8 m^3 of water to the Tarim River, accounting for 40% of the total runoff of the river (Shen et al., 2006). This particular hydrological phenomenon results in a unique baseflow mechanism in the Tarim River Basin, being sensitive to the climatic change. In addition, the permafrost in China is mostly warm permafrost, therefore is sensitive to climate change. Due to the increase of temperature, melt of permafrost along the glacier front may also contribute a certain amount of water to the groundwater and increase baseflow in the rivers. However, because no permafrost change data are available in this region, the analysis between melt of permafrost and baseflow was not performed in this study.

Studies have shown that the average temperature in the Tarim River Basin had an increasing trend over the past 50 years (Fan et al., 2011; Chen et al., 2010). This would lead to an increase of glacier melt, and consequently an increase of the surface runoff and the amount of groundwater recharge along the flow pathways, resulting in a change of baseflow pattern in the region (Fig. 5).

4.3.3. Temperature threshold for baseflow

We conducted a regression analysis between annual temperature, precipitation, and BFI. A strong relationship between BFI and temperature was found (Fig. 6). Based on the regression results, we identified temperature threshold for each river, which is the turning point where the temporal trend of BFI alters.

At the Aksu River, when the temperature is below 3 °C, the BFI increases from 47% to 87%. When the temperature ranges from 3 °C

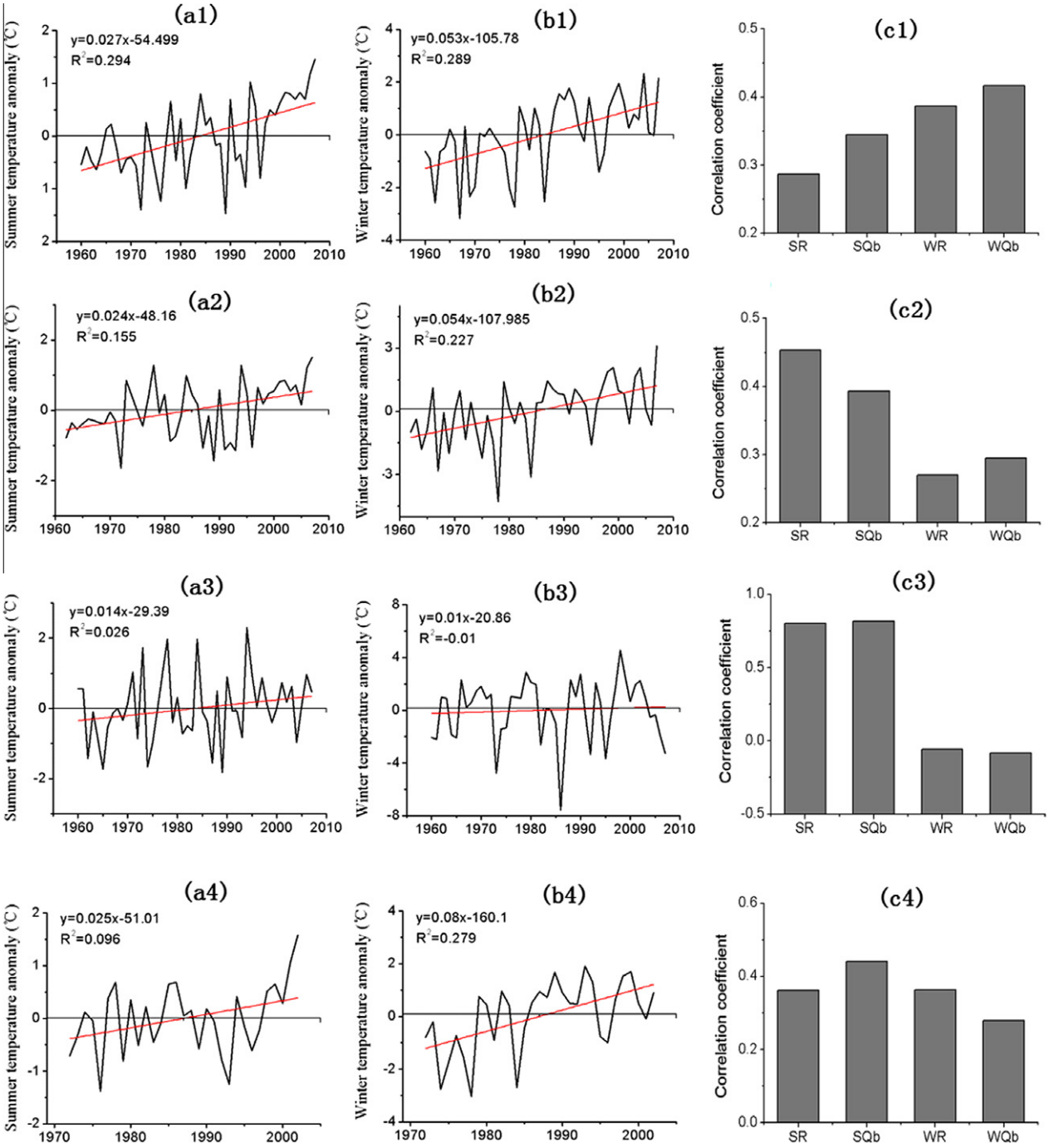

Fig. 5. Variation of summer temperature anomaly, winter temperature anomaly, and their correlations with total runoff and baseflow: (a1), (a2), (a3), and (a4) average summer temperature for the Aksu River, Hotan River, Yarkant River, and Kaidu River respectively; (b1), (b2), (b3), and (b4) average winter temperature for the Aksu River, Hotan River, Yarkant River, and Kaidu River respectively; and (c1), (c2), (c3) and (c4) correlations between summer temperature, winter temperature, and total runoff, baseflow for the headwater streams, SR: summer temperature and total runoff; SQ_b: summer temperature and baseflow; WR: winter temperature and total runoff; and WQ_b: winter temperature and baseflow.

to 20 °C, its BFI decreases from 87% to 50%. Fig. 5a1 shows that the monthly winter temperature at this river has dramatically increased during the last 50 years. This has resulted in a significant increase in evaporation, and decrease in glacier storage. The rise of temperature in all seasons causes an increase of glacier temperature, and therefore even a small increase in the summer temperature may lead to a considerable increase of glacier melt runoff, and the proportion of baseflow in the runoff would dramatically decrease. This could be a reason for that runoff and baseflow have a higher correlation with winter temperature than summer temperature in the Aksu River (Fig. 5c1). When the temperature is over 20 °C, the BFI begins to rise considerably. This is because the glacier meltwater may supply not only the surface runoff, but also contributes to the baseflow, leading to a BFI increase.

At the Hotan River, when temperature is below 4 °C, the BFI increases from 50% to 90%. When temperature ranges from 4 °C to 15 °C, its BFI decreases and the minimum can be down to 40%. When temperature is over 15 °C, its BFI begins to rise considerably. Although the Hotan River has a similar fitting curve as that for the Aksu River, its variability is less drastic (Fig. 6). This is because the

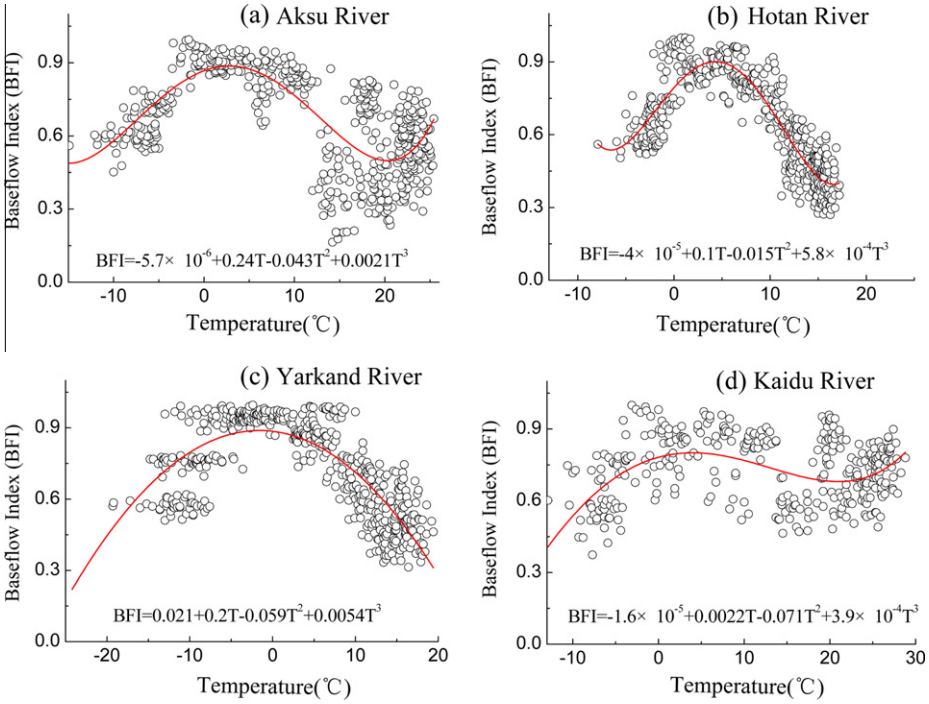

Fig. 6. Relationship between baseflow index and temperature for the four headstreams of the Tarim River.

summer temperature has a stronger relationship with the runoff and baseflow than that of the winter temperature in the Hotan River (Fig. 5c2), indicating that runoff and baseflow of the river is more sensitive to summer temperature. When summer temperature is above the average after 1989 (Fig 5a2), the BFI begins to increase significantly (Fig. 2). Among the four rivers, the Hotan River has the minimum shrinking rate of glacier area (2.1–2.5%), and the average decreasing rate of ice reserves is below 3% (Shen et al., 2006). In addition, the summer temperature of the Hotan River has a stronger relationship with the runoff than that with the baseflow, which indicates that the Hotan River receives less supply from glaciers, compared with other rivers.

The Yarkand River is quite different from the Aksu River and Hotan River. When the temperature is below 0 °C, the BFI increases until it reaches 88%. When the temperature is above 0 °C, its BFI decreases slowly down to 40%. Runoff and baseflow have stronger correlations with summer temperature than winter temperature (Fig 5c3). This may be because that the Yarkand River has a large glacier storage (the largest among the four rivers) and a large amount of runoff is from glacier meltwater. Since late 1990s, the monthly summer temperature at this river has been greater than the 50 years' average, and the baseflow has shown a same pattern (Fig 2). However, the magnitude of temperature rise of the Yarkand River Basin is fairly limited, and therefore the curve shape in Fig. 5c3 is comparable with the curves in Fig. 5a3 and b3. If temperature rises continuously its BFI should show a similar pattern to those of the Aksu River and Hotan River.

At the Kaidu River, when the temperature is below 0 °C, the BFI increases until it reaches 78%. When the temperature ranges from 0 °C to 20 °C, the BFI decreases from 78% to 70%. When the temperature is over 20 °C, the BFI increases considerably. The Kaidu River is mainly supplied by the glacier meltwater in summer. In the past 50 years, despite the considerably increasing baseflow, its BFI has shown a decreasing trend. The winter temperature in the catchment has increased considerably in the past years, causing more evaporation and less glacier deposit in winter. As a result, a small rise of temperature in summer may lead to a large amount of glacier melt (Shen et al., 2006).

5. Conclusions

The Tarim River is the largest inland river of China and a major water resource of the vast arid area in northwestern China. In this study, we used a number of methods to assess the variation of baseflow in the four major headstreams of the Tarim River in the past 50 years, and to explore possible reasons for the variation from the perspectives of climate (temperature and precipitation) and glacier melt. Our major findings are:

(1) Over the past 48 years, the increase rates of baseflow for the Aksu, Hotan, Yarkand, and Kaidu rivers are 14.1%, 6.9%, 20.1%, and 42.6%, respectively. However, the baseflow increases do not coincide with the changes of SBFI. The SBFI of the Hotan, Yarkand, and Kaidu rivers are 8.0–30.1% of the streamflow in dry years, and 10.8–37.0% in wet years. The increase of baseflow as a result of increasing glacial meltwater leads to the uncommon scenario that an increasing precipitation and a larger BFI occur in the same year.
(2) This detailed investigation of baseflow variation revealed that baseflow shows an increasing trend for all the four major headstreams of the Tarim River. As for BFI, the Aksu and Hotan rivers show increasing trends, whereas the Yarkand and Kaidu Rivers do not have monotonic trends. The major time scales of the annual baseflow for the four rivers are 3–5 years, 10–14 years, and 25 years. The lowest baseflow and seasonal factors occur in December and January; both increase gradually from February to July, and reach their maximums in July or August.
(3) The responses of runoff and baseflow to climactic factors are different. Precipitation has a great impact on runoff, whereas temperature has a great impact on baseflow. Baseflow and

glacier meltwater are both major sources of streamflow to the Tarim River. The increase of temperature will promote glacier melt, and consequently increase the amount of groundwater recharge and baseflow. Regression analyses were conducted in this study to identify the temperature thresholds in the BFI time series for the four headstreams over the past 50 years. These threshold values and regression relationships will help to assess and predict the impact of climate changes on streamflow and baseflow in the region.

Acknowledgements

This research is supported by the National Basic Research Program of China (973 Program), No. 2010CB951003. We appreciate comments provided and encouragement made by the reviewers, the editor and the associate editor.

References

Antonia, L., Paolo, V., 2008. Baseflow index regionalization analysis in a Mediterranean area and data scarcity context: role of the catchment permeability index. J. Hydrol. 355, 63–75.
Burn, D.H., 1994. Hydrologic effects of climate change in west central Canada. J. Hydrol. 160, 53–70.
Chen, Y.N., Xu, Z.X., 2005. Plausible impact of global climate change on water resources in the Tarim River Basin, China. Sci. China: Series D 48, 65–73.
Chen, L.Q., Liu, C.M., et al., 2006. Change of the Baseflow and It's Impacting Factors in the Source Regions of Yellow River. J. Glaciol. Geocryol. 28, 141–148.
Chen, Y.N., Xu, C.C., Hao, X.M., et al., 2008. Fifty-year climate change and its effect on annual runoff in the Tarim River Basin, China. J. Glaciol. Geocryol. 30, 921–929.
Chen, Y.N., Xu, C.C., Yang, Y.H., et al., 2009a. Hydrology and water resources variation and its responses to regional climate change in Xinjiang. Acta Geogr. Sinica 64, 1331–1341.
Chen, Y.N., Xu, C.C., Hao, X.M., et al., 2009b. Fifty-year climate change and its effect on annual runoff in the Tarim River Basin, China. Quatern. Int. 208, 53–61.
Chen, Y.N., Xu, C.C., Chen, Y.P., et al., 2010. Response of Glacial-lake outburst floods to climate change in the Yarkant River basin on northern slope of Karakoram Mountains, China. Quatern. Int. 226, 75–81.
Dai, Y.S., 2000. The time frequency analysis approach of electric noise based on the wavelet transform. Solid-State Electr. 44, 2147–2153.
Eckhardt, K., 2005. How to construct recursive digital filters for baseflow separation. Hydrol. Process. 19, 507–515.
Eckhardt, K., 2008. A comparison of baseflow indices, which were calculated with seven different baseflow separation methods. J. Hydrol. 352, 168–173.
Fan, Y.T., Chen, Y.N., Li, W.H., et al., 2011. Response of runoff to temperature and precipitation changes in Tarim River during the past 50 years. J. Arid Land 3, 220–230.
Fu, L.X., Chen, Y.N., Li, W.H., et al., 2010. Relation between climate change and runoff volume in the headwaters of the Tarim River during the last 50 years. J. Desert Res. 30, 204–209.
Fuente, A.D., Bing, N., Hoeschele, I., et al., 2004. Discovery of meaningful associations in genomic data using partial correlation coefficients. Bioinformatics 20, 3565–3574.
Hafzullah, A., Ilker, K., Ebru, E., 2009. Filtered smoothed minima baseflow separation method. J. Hydrol. 372, 94–101.
Hodgkins, G.A., Dudley, R.W., 2011. Historical summer baseflow and stormflow trends for New England Rivers. Water Resour. Res., W07528.
Institute of Hydrology, 1980. Low Flow Studies. Research Report, Wallingford, Oxon.
Jiang, Y., Xia, J., 2007. The hydrological characteristics of runoff and its response to climatic change in Tarim. Resour. Sci. 29, 45–52.
Jiang, Y.L., Zhou, X.H., 2007. Application study of season character exponential smoothing in using water forecasting of city. Sci. Technol. Eng. 7, 1666–1669.
Jozsef, S., Marc, B.P., 1998. Baseflow separation based on analytical solutions of the Boussinesq equation. J. Hydrol. 204, 251–260.
Liu, S.Y., Ding, Y.J., Shang, G., et al., 2006. Glacier retreat as a result of climate warming and increased precipitation in the Tarim river basin, northwest China. Ann. Glaciol. 43, 91–96.
Lyne, V.D., Hollick, M., 1979. Stochastic time-variable rainfall runoff modelling. Hydrology and Water Resources Symposium, vol. 32. Institution of Engineers, Australia, pp. 89–92.
Men, Y.M., Yan, C.G., 2002. Seasonal exponential smoothing method in groundwater level forecast. Geotech. Invest. Surv. 2, 25–27.
Mwakalila, S., Feyen, J., et al., 2002. The influence of physical catchment properties on baseflow in semi-arid environments. J. Arid Environ. 52, 245–258.
Nathan, R.J., McMahon, T.A., 1990. Evaluation of automated techniques for base flow and recession analyses. Water Resour. Res. 26, 1465–1473.
Riggs, H.C., 1964. The baseflow recession curve as an indicator of ground water. Int. Assoc. Sci. Hydrol., 352–363.
Shen, Y.P., Wang, S.P., Wang, G.Y., 2006. Response of glacier flash flood to global warming in Tarim River Basin. Adv. Clim. Change Res. 2, 32–35.
Shi, Y.F., 1990. Glacier recession and lake shrinkage indicating the climatic warming and drying trend in Central Asia. Acta Geogr Sinica 45, 1–13.
Shi, Y.F., 2005. China Glacier Inventory (CGI). Shanghai Kexuepuji Press, Shanghai, pp. 61–64.
Shi, Y.F., Xie, Z.C., 1964. The basic characteristics of the existing glaciers in China. Acta Geogr. Sinica 30, 183–208.
Sloto, R.A., Crouse, M.Y., 1996. HYSEP: A Computer Program for Streamflow Hydrograph Separation and Analysis: US Geological Survey Water Resources Investigations Report. Lemoyne, Pennsylvania: US Department of the Interior.
Szilagyi, J., 2004. Heuristic continuous base flow separation. J. Hydrol. Eng. 9, 311–318.
Szilagyi, J., Harvey, F.E., Ayers, G.F., 2005. Regional estimation of base recharge to ground water using water balance and a base-flow index. Ground Water 41, 504–513.
Tallaksen, L.M., 1995. A review of baseflow recession analysis. J. Hydrol. 165, 349–370.
Tang, Q.C., Zhang, J.B., 2001. Water resources and eco-environment protection in the arid regions in Northwest of China. Prog. Geogr. 20, 227–233.
Tetzlaff, D., Soulsby, C., 2008. Sources of baseflow in larger catchments – using tracers to develop a holistic understanding of runoff generation. J. Hydrol. 359, 287–302.
Xie, F.M., Mao, W.Y., Zhang, J.G., et al., 2007. Analysis of streamflow from four source rivers to mainstream of the Tarim River, 2005. J. Glaciol. Geocryol. 29, 559–569.
Xu, Z.X., Takeuchi, K., Ishidaira, H., 2003. Monotonic trend and step changes in Japanese precipitation. J. Hydrol. 279, 144–150.